

A New Set of LGT Constants and Temperature Coefficients Extracted Through Resonant and Pulse Echo Techniques

B. T. Sturtevant¹, P. M. Davulis², M. Pereira da Cunha²
Dept. of Physics¹ and Dept. of Electrical and Computer Engineering²
Laboratory for Surface Science and Technology
University of Maine, Orono, Maine USA
mdacunha@eece.maine.edu

Abstract— The langasite family of crystals (LGX) has received significant attention in the past ten years for acoustic wave (AW) applications due to their higher piezoelectric coefficients than quartz, the existence of temperature compensated orientations confirmed experimentally, the absence of crystalline phase transitions below their melting points, and consistency in the crystals' growth and processing for device fabrication.

In this paper, langatate (LGT) acoustic wave phase velocities have been measured using combined thickness and lateral field excitation (TFE, LFE) resonant techniques along with pulse echo measurements. The measured phase velocities are used for the extraction of room temperature elastic and piezoelectric constants along with their temperature coefficients measured in this work from 5° and 120°C. The techniques and methodology employed, the LGT extracted constants and temperature coefficients, and comparisons with existing data in the literature are discussed.

I. INTRODUCTION

The precise determination of the acoustic wave (AW) crystal constants at a reference temperature (T_{ref}), such as room temperature (T_0), is the first step in a material characterization for AW device applications. Since several of the crystal constants may not vary significantly around a certain temperature range, the incorrect determination of the reference temperature values may result in a pointless effort to the extraction of the temperature coefficients. Once the constants at T_{ref} have been determined as precisely as possible, one targets the extraction of the temperature coefficients, which allow for the prediction of AW temperature behavior along arbitrary orientations.

LGX crystals have been shown to present temperature compensated orientations for the bulk acoustic wave (BAW) and surface acoustic wave (SAW). For the LGX family of crystals, the thermal coefficients of expansion and the temperature coefficients of the elastic constants dominate the AW temperature behavior, followed by the coefficients of the dielectric and piezoelectric constants.

Material constants for langatate (LGT) can be found in [1-5], and temperature coefficients in [1,2]. One motivation for the present work was the variation between the published constants and temperature coefficients, and the mismatch between predicted temperature behavior and measured device performance [1].

In this work, two independent measurement procedures are employed for the determination of the material constants and temperature coefficients. Room temperature bulk acoustic wave (BAW) velocities were measured both by modified pulse echo overlap (PEO) and combined resonance techniques (CRT) employing both thickness and lateral field excitation (TFE, LFE). The resonance measurement setup was used to make BAW phase velocity measurements between 5° and 120° C.

A set of thirteen phase velocity values measured by CRT was used to determine the elastic and piezoelectric constants of the material at each measured temperature. As each of the constants is involved in more than one phase velocity equation, the constants were extracted from multiple equations to check for consistency. A final set of constants was then determined, which provided the minimal error between the measurements performed and the corresponding predicted phase velocity values.

The sample preparation and the techniques used for the measurement of BAW phase velocity are described in **Section II**. **Section III** describes the method used to extract the material constants from the measured BAW phase velocity values. **Section IV** presents and discusses the measured results, while **Section V** concludes the paper.

II. EXPERIMENTAL TECHNIQUES

A. Sample Preparation

The LGT samples used in this work for both the PEO measurements and the CRT measurements have been designed and fabricated in the Microwave Acoustic Materials

Funding for this project was provided by the Army Research Office ARO Grant # DAAD19-03-1-0117, by the Petroleum Research Fund Grant ACS PRF# 42747-AC10, and by National Science Foundation NSF Grant # DGE-0504494.

Laboratory (MAML) at the University of Maine (UMaine). The LGT boule used in this work was purchased from (Fomos OAS, Moscow, Russia). The sample alignments along crystalline and rotated axes were done by X-ray diffraction (XRD) techniques using a Scintag X2 Advanced Diffraction System (Scintag/Thermo Electron Corp., Waltham, MA) and more recently with a PANalytical X'Pert PRO MRD (PANalytical Inc., Natick, MA) using an alignment procedure described in [6]. The samples were cut using an inner diameter saw (Meyer-Berger, Steffisberg, Switzerland). Employing the equipment and techniques mentioned, sample alignment and cut better than a few minutes have been obtained at UMaine. The samples were then ground and polished to an optical finish. The dimensions of all samples were determined through repeated measurements using a precision length gauge (Heidenhain Corporation, Schaumburg, IL).

For the PEO measurements performed in this work two types of parallelepipeds have been fabricated. One of the parallelepipeds has its faces normal to crystalline axes X, Y, and Z, whereas the second type has one face normal to crystalline axis X and the other faces normal to $\pm 45^\circ$ Y-rotated orientations. The parallelepiped dimensions were designed to avoid pulse overlap and to minimize spurious reflections due to power flow angle of various modes when used with a 2" long fused silica buffer rod [7]. The dimensions of the parallelepiped used for the X, Y, Z modes was 15.0, 20.7, 21.6 mm³ (X, Y, Z). The relevant dimensions for the parallelepiped used for the Y rotated modes was 21.7, 21.8 mm² (Y+45, Y-45).

For the CRT measurements, plates ranging in thickness from 400 μ m to 700 μ m have been aligned, cut, and optically polished at UMaine's MAML. The chosen thickness range of the wafers is a compromise between observing fabrication limits, having wafers thin enough to measure clean resonances, and having wafers thick enough to be able to measure the thickness with an acceptably low ($\approx 10^{-3}$) relative uncertainty.

B. Pulse Echo

Fourteen modes of BAW phase velocity were measured using a modified pulse echo method [8]. A schematic of the experimental apparatus for the PEO method is shown in Fig. 1a. The phase velocity of the three independent BAW modes along X, Y and two Y rotated cuts (Y $\pm 45^\circ$, Euler angles $[\Phi, \Theta, \Psi] = [0^\circ, \pm 45^\circ, 90^\circ]$) and the two independent Z modes were measured.

The BAW modes were excited by lithium niobate (LNO) transducers excited with a RITEC RAM-5000 pulse generator (Ritec Inc., Warwick, RI) into a 2" fused silica buffer rod. The LNO transducers were designed to have a fundamental frequency around 6 MHz. A 36 $^\circ$ Y rotated LNO cut was used for excitation of longitudinal modes and a 163 $^\circ$ Y rotated LNO cut was used for shear mode generation. The fused silica buffer rod was placed between the transducer and the sample (Figs. 1a and 1b) and designed to serve the double purpose of clearly identifying the reflection from the face of the sample abutting the buffer rod and mitigating pulse overlapping from other modes.

The reflections of the AW from the ends of the buffer rod and from the far face of the sample were digitized and recorded using a Lecroy Wavepro 7100 oscilloscope (LeCroy Corporation, Chestnut Ridge, NY). The waveforms were loaded into MATLAB (MathWorks, Natick, MA) where successive reflections were overlapped and the delay between them was determined. A couplant correction previously reported in [8] was applied to the delay between successive reflections to determine the actual time of flight of the AW in the sample. The time of flight was used along with the measured sample dimensions to calculate the AW phase velocity for the 14 different acoustic modes.

C. Resonance Measurements

CRT utilizing both LFE and TFE of unmetallized wafers [9,10] was used in this work. The usage of unmetallized resonators in this technique attempts to minimize non-uniform distribution of motion (NUDM) effects, which have been shown to lead to measurable discrepancies in the extracted piezoelectric constants [9]. CRT also lends itself nicely to measurements at different temperatures because there is no metallization or acoustic coupling agent whose properties would change with temperature. The frequencies of interest in these measurements are the LFE resonant (f_R) and TFE antiresonant (f_{AR}) which are related to the BAW velocity, v_p , by $f_{AR/R} \lambda = v_p$, where $\lambda = 2 \cdot (\text{wafer thickness})/n$ for the n^{th} harmonic.

The LFE test fixture consists of semi-circular electrodes etched on a circuit board atop which the sample sits [10] as shown in Fig. 2a. The TFE test fixture, shown in Fig. 2b, consists of two modified General Radio 874 open circuit loads with custom machined parts. The relative separation of the electrodes is changed by screwing or unscrewing the connectors. The LFE resonant and TFE antiresonant frequencies were measured using an Agilent 4396B network analyzer with an 85046A S-parameter test set (Agilent Technologies, Inc., Palo Alto, CA).

Thirteen BAW modes were measured using five LGT plates oriented along crystalline axes X, Y, Z, and $\pm 45^\circ$ Y rotated cuts. One less mode than the PEO method was measured, since CRT does not allow the excitation of the Z longitudinal BAW mode. For each mode, as many harmonics as were identifiable were recorded. The normalized

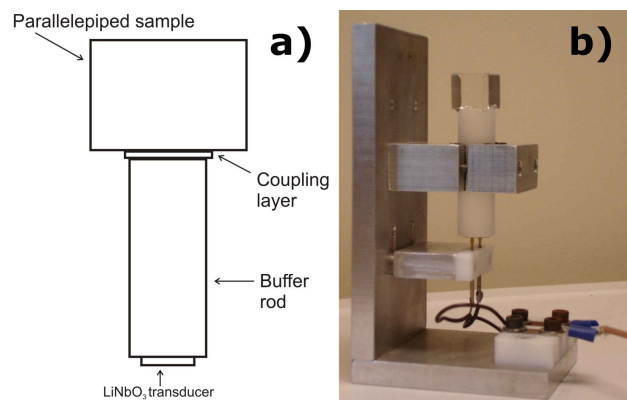


Figure 1. Pulse echo overlap measurement setup, a) schematic, b) actual fixture

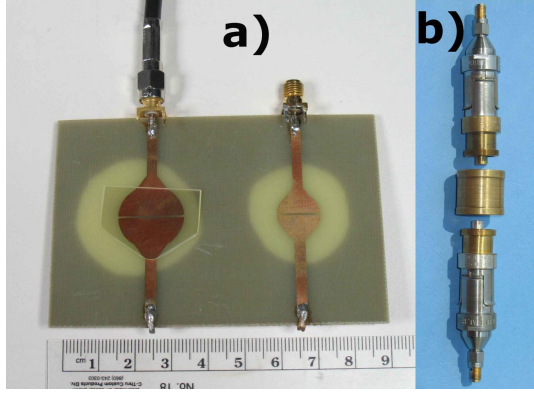


Figure 2. Resonance measurement fixtures, a) lateral field excitation, b) thickness field excitation

frequencies ($f_{AR/R/n}$) for all measured harmonics were compared and an average taken of those that converged as the $f_{AR/R}$ for that mode. These frequencies, along with the measured thickness of the wafers, were then used to determine the AW plane wave velocities, as indicated in a previous paragraph.

D. Permittivity Measurements

The two independent relative dielectric constants, ϵ_{11}/ϵ_0 and ϵ_{33}/ϵ_0 , with ϵ_0 the dielectric permittivity in vacuum, were determined through capacitance measurements of multiple circular capacitors of varying radius. Both X and Y cut wafers were used in the determination of ϵ_{11} and a Z cut wafer was used for determining ϵ_{33} . Effects of fringing electric fields were assumed to be proportional to the circumference of the capacitors [11]. Through the use of capacitors of multiple radii, these fringing effects were estimated and used to correct capacitance measurements for the determination of the permittivity constants.

III. EXTRACTION TECHNIQUE

A. Extraction of Room Temperature Constants

The phase velocity values of 14 (13) BAW modes for PEO (CRT), along with values for the density [12] and dielectric constants, were used to determine an initial ‘best guess’ at values for the elastic and piezoelectric constants. Table I outlines the process by which the phase velocities were used to determine the material constants. The nomenclature for the BAW phase velocities in the table are as follows: X, Y, Z, Y \pm 45 $^\circ$ denotes the direction of wave propagation and L, FS, SS describes the mode of propagation, respectively longitudinal or quasi-longitudinal, fast shear or quasi fast shear, and slow shear or quasi-slow shear. Because the Z-longitudinal mode is not measurable using CRT, the extraction of C_{33} via the Z-L mode could only be accomplished with the PEO technique.

As can be seen from Table I, many of the constants were extracted through several different combinations of modes. The values of the constants extracted through different combinations of velocities were cross checked for consistency and the final values constitute those which minimized the

TABLE I. METHOD OF ELASTIC CONSTANT EXTRACTION FOR A CLASS 32 CRYSTAL

Constants (in order of extraction)	Method of extraction (BAW modes and other constants used)
C_{44}	ZS
C_{66}	XFS & XSS using C_{44}
C_{11}	YL & YFS using C_{44}
e_{11}	XL with C_{11} & ϵ_{11} YSS using C_{66} & ϵ_{11}
C_{14}	XFS & XSS using C_{44} & C_{66} YL & YFS using C_{11} & C_{44}
C_{33}	ZL Y-45L & Y-45FS using C_{11} , C_{44} , C_{14} Y+45L & Y+45SS using C_{11} , C_{44} , C_{14}
C_{13}	Y-45L & Y-45FS using C_{11} , C_{44} , C_{14} , C_{33} Y+45L & Y+45SS using C_{11} , C_{44} , C_{14} , C_{33}
e_{14}	Y+45FS using C_{14} , C_{44} , C_{66} , ϵ_{11} , ϵ_{33} , e_{11} Y-45SS using C_{14} , C_{44} , C_{66} , ϵ_{11} , ϵ_{33} , e_{11}

norm between the predicted and actual measured BAW phase velocities.

The effect of the piezoelectric constants on the phase velocity of the stiffened modes is on the order of a few percent. Due to their small effect on the measured phase velocities, the extraction of the piezoelectric constants through the method outlined in the table presents a challenge. An optimization technique was thus conducted to refine the determined values of material constants. The elastic and piezoelectric constants were independently varied from the values extracted through the process outlined in Table I. The bounded search tried permutations of elastic and piezoelectric values within different bounded limits. Search monitoring ensured that the optimization routine never chose constants at the limiting bounded values (if this happened, the procedure was aborted and re-started with new initial values and wider bounded ranges).

B. Extraction of Temperature Coefficients

Phase velocities were measured at seven temperatures between 5 $^\circ$ and 120 $^\circ$ C using the resonance technique. At each measured temperature, a set of elastic and piezoelectric constants was determined by the procedure described in Sections II and III. Each constant was then plotted versus temperature and the temperature coefficients, TC1 and TC2 were extracted from a second order polynomial fit to the measured data. The value of a material constant at a temperature, T , is then expressed by the expansion:

$$X_{ij}(T) = X_{ij}(25) * \sum_{n=0}^2 (T-25)^n * TCn; \quad (1)$$

where X_{ij} is a material constant (C_{ij} , e_{ij} , or ϵ_{ij}), and $TC0=1$.

IV. EXPERIMENTAL RESULTS

A. Room Temperature Measurements

The room temperature phase velocity measurements made with PEO and CRT are compared in Table II. The agreement between the BAW phase velocities measured through the PEO and CRT is 11 parts in a thousand in the worst case and about

TABLE II. MEASURED VELOCITY COMPARISON

Propagation Direction	Mode	Measured Velocities (25°C)		
		CRT	PEO	% Diff.
X	L	5563.9	5576.2	0.22%
	FS	3136.0	3138.5	0.08%
	SS	2244.5	2251.5	0.31%
Y	L	5508.0	5556.5	0.88%
	FS	2816.5	2847.0	1.08%
	SS	2591.1	2608.7	0.68%
Z	L	Not Measurable	6527.1	---
	S	2884.2	2884.0	-0.01%
Y+45	L	5809.2	5776.0	-0.57%
	FS	3088.2	3109.7	0.69%
	SS	3054.3	3083.5	0.95%
Y-45	L	6068.4	6104.9	0.60%
	FS	3157.1	3169.5	0.39%
	SS	2285.5	2290.7	0.23%

a. Percent Difference = $(V_{PEO} - V_{CRT})/V_{PEO} * 100\%$

5 parts in a thousand when all modes are averaged. The relative error in both the PEO and CRT velocity measurements was primarily attributed to the precision with which the parallelepiped and plate thickness dimensions could be measured. The much larger dimensions of the PEO parallelepiped samples led to relative uncertainty in the acoustic path length of better than $2 * 10^{-4}$, while the relative uncertainty of the thickness of the resonant plate was better than $5 * 10^{-3}$.

For the CRT measurements, odd numbered resonant frequencies, typically between $n=1$ and $n=11$, were measured and compared to determine f_{ARR} for each mode. It was found experimentally that the fundamental frequency was higher than the normalized higher harmonics in every case and was thus not used in the averaging for the interpretation of the resonance data. For a typical mode, f_{ARR} represents an average of odd harmonics 3 through 11. For the plates fabricated, odd harmonics up to the nineteenth were able to be recorded for some orientations, such as the Y-45 L mode, while only harmonics 1 to 5 were able to be identified and recorded for other orientations, such as the Y-45 FS mode.

The final set of constants found through the optimization procedure described in Section III decreased the norm of the vector defined by the difference between the measured phase velocities and the phase velocities predicted by the extracted constants by 84% for the PEO data and 71% for the CRT data. The optimized constants found through PEO and CRT are compared in Table III and can be seen to agree well, with the largest difference in elastic constants being 3.5% for C_{13} . The large difference between the values for e_{14} extracted by PEO and CRT reflects the reduced influence that this constant has in the BAW modes measured and thus the difficulty of extracting it through the methods described in this paper. Because the absolute norm of the difference vector was four times lower for the PEO data than for the CRT data, the constants extracted by the PEO measurements were used as the measured room temperature constants. The constants extracted from the PEO velocity measurements through the procedure described above are compared with those published in the literature for room temperature in Table IV. As can be seen from Table IV, values for C_{13} existing in the literature fall into two different ranges of values with one range about 102

GPa, the other being close to 127 GPa. Our determined value for C_{13} , 100.63 GPa, fits the first group.

B. Determination of Temperature Coefficients

Efforts in employing the PEO technique at temperatures higher than a few tens of degrees centigrade indicated that the properties of the acoustic couplant used to bond the sample to the buffer rod changed significantly with temperature. Thus, variations in the crystal material properties with temperature were obscured by the couplant behavior. The resonance experiments, on the other hand, did not have any coupling or material deposited on the devices. As a result, the CRT was more attractive for extracting the temperature coefficients and therefore employed in this work. Because the temperature coefficients are reflective of changes normalized to a value at a particular reference temperature, the extraction of these coefficients from the CRT data was consistent with the use of PEO values at room temperature.

The temperature coefficients for the material constants were determined using the procedure described above and are presented in Table V. As seen in Table V, C_{44} and C_{66} are much less sensitive to temperature changes than the other constants, with C_{44} for instance decreasing by only one part in a million per degree Celsius. On the other hand, C_{13} and C_{33} vary about two orders of magnitudes more to first order.

TABLE III. ROOM TEMPERATURE CONSTANTS AFTER NUMERICAL FITTING

	CRT	PEO	% Diff
C_{ij}^E (GPa)			
C_{11}^E	188.54	189.41	-0.5%
C_{12}^E	108.98	109.06	-0.1%
C_{13}^E	100.43	100.63	-0.2%
C_{14}^E	13.13	13.60	-3.5%
C_{33}^E	264.63	262.29	0.9%
C_{44}^E	50.49	51.12	-1.2%
C_{66}^E	39.78	40.17	-1.0%
e_{ij} (C/m ²)			
e_{11}	-0.482	-0.518	-7.2%
e_{14}	0.167	0.051	106%

TABLE IV. ELASTIC AND PIEZOELECTRIC CONSTANTS (25°C)

	This Work	[1]	[2]	[3]	[4]	[5]
C_{ij}^E (GPa)						
C_{11}^E	189.41	188.60	202.00	189.40	188.90	188.81
C_{12}^E	109.06	107.90	120.00	108.40	108.60	107.84
C_{13}^E	100.63	103.40	125.00	132.00	104.40	100.15
C_{14}^E	13.60	13.50	13.30	13.70	13.74	13.50
C_{33}^E	262.29	261.90	288.00	262.90	264.50	261.05
C_{44}^E	51.12	51.10	49.70	51.25	51.29	50.95
C_{66}^E	40.17	40.30	40.70	40.52	40.19	40.49
e_{ij} (C/m ²)						
e_{11}	-0.518	-0.456	-0.468	-0.54	0.508	-0.478
e_{14}	0.051	0.094	0.0632	0.07	-0.028	0.043
$\epsilon_{ij}^S / \epsilon_0$						
$\epsilon_{11}^S / \epsilon_0$	17.95	18.3	19.3	17.5	19.6	19.1
$\epsilon_{33}^S / \epsilon_0$	75.14	78.9	60.9	76.5	80.3	78.1

REFERENCES

TABLE V. EXTRACTED TEMPERATURE COEFFICIENTS ($T_{REF} = 25^\circ$)

	TC1 ($10^{-6} \text{ }^\circ\text{C}^{-1}$)	TC2 ($10^{-9} \text{ }^\circ\text{C}^{-2}$)
C_{11}^E	-71.2	-96.1
C_{12}^E	-138.4	-50.6
C_{13}^E	83.8	-1045.1
C_{14}^E	-362.1	48.7
C_{33}^E	-85.1	12.5
C_{44}^E	-1.0	-55.9
C_{66}^E	15.1	-154.4
ϵ_{11}	-33.6	969.9
ϵ_{14}	-32.2	-32014.1

V. CONCLUSIONS

This paper has reported on the extraction of LGT room temperature acoustic wave elastic, dielectric and piezoelectric constants and their respective temperature coefficients from 5 to 120°C. Two techniques have been used in this work, namely the pulse echo overlap and the combined thickness and lateral field excitation resonance measurements. The procedure used for the extraction of the elastic and piezoelectric constants from a representative set of phase velocity measurements has been described.

The measured constants obtained are in general agreement with the literature and reflect the maturity of LGT as an acoustic wave material. Consistent results have been observed between the two techniques, with discrepancies for both measured BAW phase velocities and extracted elastic constants better than a few percent when comparing PEO and CRT. The PEO technique showed more consistent results at room temperature whereas the CRT technique showed better performance in extracting the temperature coefficient of the elastic and piezoelectric constants due to the absence of any perturbation on the sample to be tested. From the measurements performed, first and second order temperature coefficients have been extracted and reported in this work.

ACKNOWLEDGMENT

The authors would like express their gratitude to the personnel from the Laboratory of Surface Science and Technology (LASST) and Dept. of Electrical and Computer Engineering for valuable technical discussion and for cutting and polishing most of the samples used in this work.

- [1] M. Pereira da Cunha, D. C. Malocha, E. L. Adler, K. J. Casey, "Surface and pseudo surface acoustic waves in langatate: predictions and measurements," IEEE Trans. Ultrason., Ferroelect., Freq. Cont., vol 49, pp 1291-1299, September 2002.
- [2] N. Onozato, M. Adachi, T. Karaki, "Surface acoustic wave properties of La₃Ta_{0.5}Ga_{5.5}O₁₄ single crystals," Jpn. J. Appl. Phys., vol 39, pp 3028-3031, May 2000.
- [3] Y. V. Pisarevsky, P.A. Senyushenkov, B.V. Mill, N.A. Moiseeva, "Elastic, Piezoelectric, Dielectric Properties of La₃Ga_{5.5}Ta_{0.5}O₁₄ Single Crystals," Proc. 1998 IEEE Int'l. Freq. Cont. Symp., pp 742-747.
- [4] J. Bohm, E. Chilla, C. Flannery, H.J Frohlich, T. Hauke, R.B. Heimann, M. Hengst, U. Straube, "Czochralski growth and characterization of piezoelectric single crystals with langasite structure: La₃Ga₅SiO₁₄ (LGS), La₃Ga_{5.5}Nb_{0.5}O₁₄ (LGN) and La₃Ga_{5.5}Ta_{0.5}O₁₄ (LGT) II. Piezoelectric and elastic properties," Journal of Crystal Growth, 216, pp 293-298, 2000.
- [5] J. Schreuer, "Elastic and piezoelectric properties of La₃Ga₅SiO₁₄ and La₃Ga_{5.5}Ta_{0.5}O₁₄: an application of resonant ultrasound spectroscopy," IEEE Trans. Ultrason., Ferroelect., Freq. Cont., vol 49, pp 1474-1479, November 2002.
- [6] L. D Doucette, M. Pereira da Cunha, R. J. Lad, "Precise orientation of single crystals by a simple x-ray diffraction rocking curve method," Rev. Sci. Instr., vol. 76, 036106 (4 pages), 2005.
- [7] B. J. Meulendyk, M. Pereira da Cunha, "Significance of power flow angle interference due to finite sample dimensions in reflection measurements," Proc. 2005 IEEE Int'l. Freq. Cont. Symp., pp 164-170.
- [8] B.T Sturtevant, M. Pereira da Cunha, "BAW phase velocity measurements by conventional pulse echo techniques with correction for couplant effect," Proc. 2006 IEEE Int'l Ultrason. Symp., pp 2261-2264.
- [9] J. Kosinski, A. Ballato, and Y. Lu, "A Finite Plate Technique for the determination of piezoelectric material constants," IEEE Trans. Ultrason., Ferroelect., Freq. Contr., vol. 43, no 2, pp. 280-284, March 1996.
- [10] P. Davulis, J. A. Kosinski, M. Pereira da Cunha, "GaPO₄ stiffness and piezoelectric constants measurements using the combined thickness excitation and lateral field technique," Proc. 2006 IEEE Int'l Freq. Cont. Symp., pp 664-669.
- [11] V. E. Bottom, "Dielectric constants of quartz," J. Appl. Phys., vol. 43., pp 1493-1495, April, 1972.
- [12] T. R Beaucage, E.P Beenfeldt, S.A Speakman, W.D Porter, E.A. Payzant, M.Pereira da Cunha, "Comparison of high temperature crystal lattice and bulk thermal expansion measurements of LGT single crystal," Proc. 2006 IEEE Int'l Freq. Cont. Symp., pp 658-663.